

# High-Resolution Muography Using a Prototype Portable Muon Telescope

R. Perez,<sup>a)</sup> S. A. Shanto, M. Moosajee, and S. Cano<sup>b)</sup>

*Texas Tech University, Department of Physics & Astronomy,  
Advanced Particle Detector Laboratory,  
1204 Gilbert Drive, Lubbock, Texas 79416-2104, USA*

<sup>a)</sup> Corresponding author: raulperezjr.perez@ttu.edu

<sup>b)</sup> samuel.cano@ttu.edu

**Abstract.** We report on our continued development of a portable muon telescope with excellent angular resolution capable of imaging large archaeological structures in detail. The first prototype (Phase I) consists of four trays of scintillator bars, Winston cones, silicon photomultipliers (SiPMs), readout electronics, and a network of Arduinos to handle data acquisition. Finally, we developed a reconstruction algorithm to create the final image. The cosmic muons produce scintillation photons as they pass through the scintillator bars; these photons are transported by the Winston cones to the SiPMs where they are converted into electrical signals. The electrical signals are then digitized and transmitted to an offline computer for reconstruction. The entire system is mounted on a wheeled cart and can be pointed to target different objects of interest. With Phase I, we are able to reconstruct large objects in two-dimensional space with an angular resolution of 20 mrad with an operating efficiency of 89%.

## INTRODUCTION

Muons are elementary particles able to penetrate deep into structures, allowing us to image through very dense material. The muons we interact with are created in the Earth's upper atmosphere from cosmic rays colliding with the nuclei of air molecules. These high-energy collisions result in pions, which often decay into muons and muon neutrinos.<sup>1</sup> The muon flux reaching the Earth's surface is about 10,000 muons per minute per square meter, making them the most abundant cosmic ray particle at sea level.<sup>2</sup> These charged particles lose energy mostly through inelastic collisions in materials. Many of these collisions can take place per given path length, causing substantial energy loss. The energy loss per unit length ( $-dE/dx$ ) is generally given by the Bethe-Bloch formula<sup>3</sup> and is used to describe the density-dependent energy loss in materials. Muon tomography is a technique that uses this fact and the measured muon flux to reconstruct images. Muon tomography has been used to image large objects such as volcanoes, buildings, and ancient archaeological structures for more than 50 years.<sup>4</sup> In his pioneering work, Alvarez searched for hidden structures in an Egyptian pyramid in 1970, thus showing the noninvasive feature of muon tomography and its applications.<sup>5</sup>

The goal of this project is to develop a portable muon telescope that is capable of the best possible angular resolution that is physically attainable. Developing such a system requires an efficient muon detector, communication electronics, and excellent software for reconstructing the muon trajectory. Our first prototype telescope (Phase I) was built at the Advance Particle Detector Lab at Reese Technology Center in the summer of 2019 for training purposes. In this paper, we discuss the performance, detector construction, and results from imaging a local water tower using the Phase-I telescope.

## Phase-I Muon Telescope

The Phase-I telescope is mounted on an aluminum frame cart, spanning an area of approximately  $90 \text{ cm} \times 180 \text{ cm}$ , as shown in Fig. 1(a). The telescope consists of four trays of plastic scintillator bars (Eljen, EJ-200).<sup>6</sup> Each bar has a cross-sectional area of  $5 \times 5 \text{ cm}$  and is 60 cm long. Every other tray is rotated by 90 degrees so that the bars in adjacent trays are perpendicular. Measuring a signal in a pair of consecutive trays allows both  $x$  and  $y$  position of the incident muon to be inferred. The two pairs of trays give independent  $x$  and  $y$  measurements and form a track—a parameterization of the muon's trajectory. The two pairs of trays are one meter apart, providing an angular resolution of 20 mrad. The angular resolution depends on the point position resolution of a single bar (14.4 mm) and the separation distance between the two pairs of trays.

Inside each tray, 11 bars are placed parallel to each other and are individually wrapped in reflecting foil to increase the light collection efficiency of the scintillator. Figure 1(b) shows these bars in a single tray during construction. A SensL (MicroFC-60035-SMT)<sup>7</sup> silicon photomultiplier (SiPM) is optically coupled to a single bar via solid Winston cone,<sup>8</sup> which helps focus scintillation light from the larger cross-sectional area of the bars ( $5 \times 5 \text{ cm}^2$ ) to the smaller area of the SiPM ( $36 \text{ mm}^2$ ).

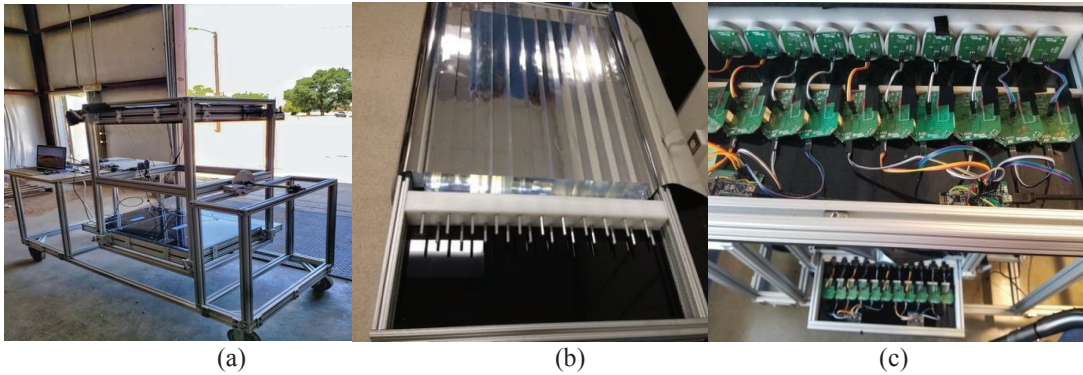


**FIGURE 1.** (a) The Phase-I muon telescope with top and bottom trays. (b) Scintillator bars positioned in a tray during construction. (c) SiPMs and custom electronics mounted to the bars in top and bottom trays.

Scintillation light is produced as a muon passes through the scintillator, losing  $\sim 2 \text{ MeV}$  per centimeter. This scintillation light is detected by a SiPM that converts photons into low-voltage pulses. Since the response time of a raw pulse from a SiPM ( $\sim 100 \text{ ns}$ ) is three orders of magnitude smaller than the time sensitivity of our readout electronics, we made a custom printed circuit board (PCB) based on MIT's Cosmic Watch,<sup>9</sup> which amplifies and stretches the raw signal. A schematic of our circuit is shown in Fig. 2. The amplified signals from a channel are then sent to an Arduino Nano, which converts them into digital signals. This task is accomplished by a pair of nanos in each tray acting as nodes, communicating with up to six channels at a time. This digitized signal is then transferred to a local computer that aggregates data from all the channels for analysis. The data acquisition software allows continuous online monitoring for data loss or hardware malfunction during a data-taking period.

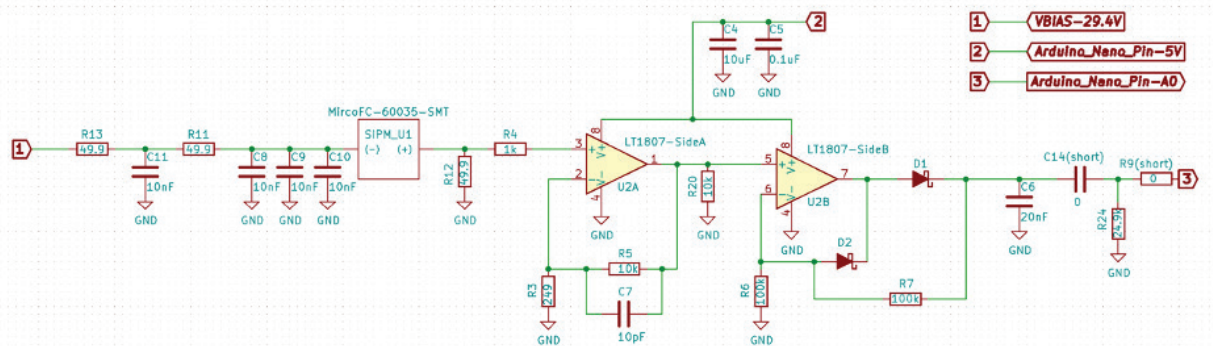


**FIGURE 2.** Schematic of circuit including SiPM.

The digitized data from a completed run are stored on a local computer for offline analysis. Our analysis requires that a muon pass through each of the four layers within a millisecond. This enables us to record two single space points— $(x, y, z = d)_T$  on the top and  $(x, y, z = 0)_B$  on the bottom—from which we can calculate the angle of impact of the muon. We store the number of muons per detected angle and their energy deposits, respectively, which allows us to reconstruct a two-dimensional image of the object of interest.

## Water Tower Experiment

Using the Phase-I telescope at Reese Technology Center, we imaged a nearby water tower as our first case study. The telescope was positioned pointing directly at the water tower at 45 degrees (Fig. 3). This configuration was empirically found to be the optimal angle for detecting the midpoint of the tank, which was defined by the location of the telescope stationed in a nearby barracks. To establish the muon flux without obstructions, reference runs were taken pointing the telescope away from the water tower. The water tower has a height and diameter of 43.8 m and 15 m, respectively, with a capacity of 500,000 gallons.

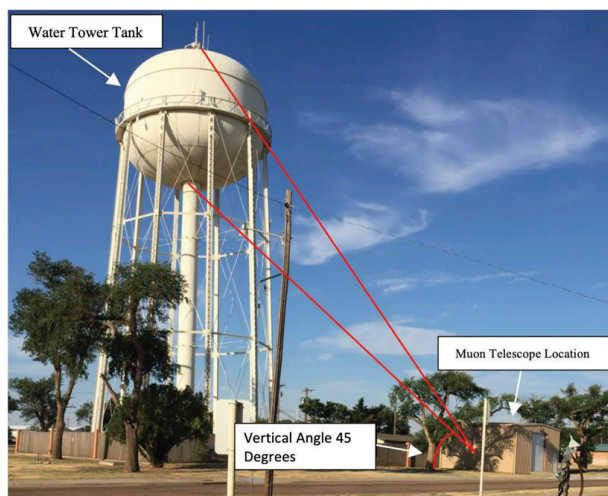


**FIGURE 3.** Water tower at the Reese Technology Center and the location of the Phase-I muon telescope.

The experiment was conducted over the course of a few months while collecting data each consecutive day for an exposure time of 24 hours. Information on the varying water levels inside the tank throughout the day was provided by Reese Technology Center personnel. A Monte Carlo simulation was created using GEANT4<sup>9,10</sup> that allowed us to model the geometry of our telescope and water tower, as shown in Fig. 4, while also allowing us to simulate how muons interacted with the materials in our models. In order to realistically describe the cosmic muon momentum spectrum, we used the Cosmic Ray Shower Library (CRY).<sup>11</sup> The program CRY is linked with GEANT4, which

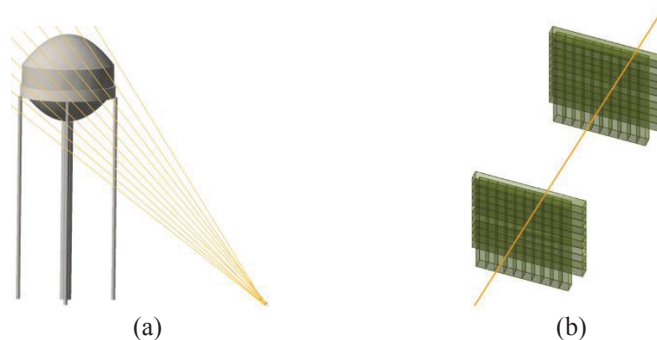


**FIGURE 4.** (a) Screen capture of detected muon tracks passing through the water tower. (b) Muon track passing through simulated scintillator bars.

allowed us to extract the relevant physical information from the muon paths as they pass through the different geometries. Muons are simulated with random trajectories, and based on whether or not they interact with our telescope model, we can infer what fraction of muons will be detected. Example trajectories of muons detected are shown in Fig. 5(a).

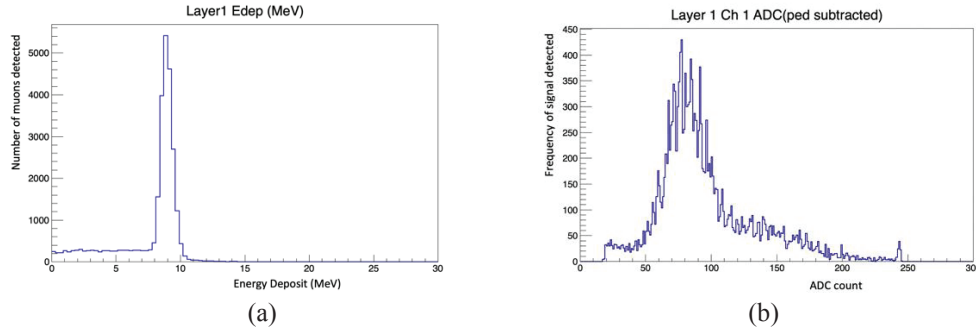


**FIGURE 5.** (a) Energy loss by muons in a single bar. (b) Measured signal distribution for a single bar in ADC counts.

During the experiment, we collected  $\sim 3$  million events during each run, with only 5.2% containing enough hits to form a muon track. Image reconstruction uses the muon tracks from both the reference run and the water tower run for the same exposure time. These two datasets contain information on the number of muons detected per a given angle. Taking the ratio between the datasets represents the color, as shown in Fig. 6(a) of our reconstructed 2D image of the water tank with respective horizontal vs. vertical axes. The ratio indicates that there is roughly a 15% loss of muons due to the presence of the water tower. This muon loss represents the muon absorption and scattering when interacting with dense materials. Similarly, we produced the same 2D image using simulated events, as shown in Fig. 6(b). The simulation suggests a 70% loss, compared to 15%. The disagreement between observation and simulation is currently being studied.

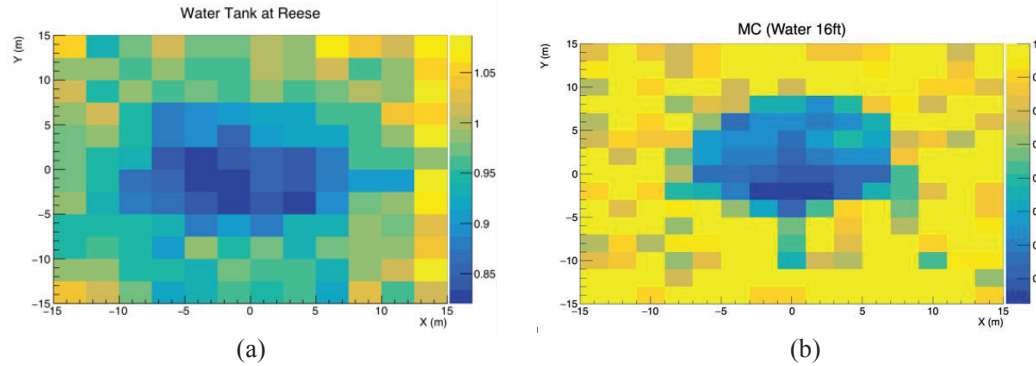


**FIGURE 6.** (a) 2D image of the water tank from data. (b) 2D image of the water tank from simulation.

## CONCLUSIONS

Our experiment shows that we can noninvasively image objects of interest using cosmic muons. The shadow of the water tank observed by our Phase-I telescope capable of an angular resolution of 20 mrad confirms that high-resolution tomography is feasible while providing portability. A comparison between the observed data and the simulation estimates the working efficiency of our telescope to be 89%. The questions of extracting the water level from the images and the disagreement between data and the Monte Carlo simulations are currently being investigated, and improvements to the system are now being implemented. The next data-taking period with the Phase-I telescope will take place this summer with significantly enhanced signal detection efficiency. We are also experimenting with

scintillator fibers as a potential replacement of scintillator bars for finer spatial segmentation. Our goal is to achieve a resolution of 0.5 mrad with the next prototype (Phase II).

## ACKNOWLEDGMENTS

The authors want to express their gratitude to Dr. Shuichi Kunori and Dr. Nural Akchurin for their guidance, help, and support. They also acknowledge contributions from Phil Cruzan (TTU), P. Przewłocki and K. Frankiewicz (MIT), the Center for Transformative Undergraduate Experiences (TrUE) at Texas Tech University, and Reese Technology Center.

## REFERENCES

- [1] S. Procureur *et al.*, Nucl. Instrum. Methods Phys. Res., Sect. A **878**, 169–179 (2018).
- [2] H. Yang *et al.*, Final Technical Report: Imaging a Dry Storage Cask with Cosmic Ray Muons, US DOE, Office of Scientific and Technical Information (2018).
- [3] M. Tanabashi *et al.* (Particle Data Group), Phys. Rev. D **98**, 030001 (2018), and 2019 update, available at <http://pdg.lbl.gov/2019/reviews/rpp2019-rev-passage-particles-matter.pdf>.
- [4] H. Gómez *et al.*, Nucl. Instrum. Methods Phys. Res., Sect. A **936**, 14–17 (2019).
- [5] L. W. Alvarez *et al.*, Science **167**, 832–839 (1970).
- [6] See supplementary material at <https://eljentechnology.com/products/plastic-scintillators/ej-200-ej-204-ej-208-ej-212> for properties and chemical compatibility of the Eljen Technology scintillator bars EJ-200.
- [7] See supplementary material at [https://sensl.com/downloads/ds/PB-Intro\\_to\\_SiPM\\_2\\_Pages.pdf](https://sensl.com/downloads/ds/PB-Intro_to_SiPM_2_Pages.pdf) for properties of the SensL SiPM.
- [8] J. A. Aguilar *et al.*, Astropart. Phys. **60**, 32–40 (2015).
- [9] See supplementary material at <https://www.analog.com/media/en/technical-documentation/data-sheets/18067fc.pdf> for properties of the amplifier.
- [10] S. Agostinelli *et al.*, Nucl. Instrum. Methods Phys. Res., Sect. A **506**, 250–303 (2003).
- [11] C. Hagmann *et al.*, Cosmic-ray Shower Library (CRY), Lawrence Livermore National Laboratory (2012), available at [https://nuclear.llnl.gov/simulation/doc\\_cry\\_v1.7/cry.pdf](https://nuclear.llnl.gov/simulation/doc_cry_v1.7/cry.pdf).